Wulfenia **19** (2012): xx–xx

Wulfenia
Mitteilungen des
Kärntner Botanikzentrums
Klagenfurt

Embryology of *Talinum paniculatum* (Jacq.) Gaertn. and *T. triangulare* (Jacq.) Willd. (Portulacaceae s.l., Caryophyllales)

Tatiana D. Veselova, Khalima Kh. Dzhalilova,
Margarita V. Remizowa & Alexander C. Timonin

Summary: We investigated embryology of two species of the genus *Talinum* in comparison with closely related taxa. Embryological data are ambivalent regarding segregation of the separate family Talinaceae. Indeed, uniseriate archesporium of the anther, thick pollen tubes that remain visible long after fertilization, uniseriate 4-celled proembryo, Solanad-type of embryo development, multinucleate endospermal haustorium are all traits typical of *Portulaca*. Therefore, embryology indicates close affinity between *Talinum* and *Portulaca*. However, the structure of exotesta in *Talinum* is nearly identical to that in *Claytonia* (Montiaceae) and *Pleuropetalum* (Amaranthaceae), both families being distantly related to the Portulacaceae s. str. The species investigated are diverse in structure of seed coat, aril and funicle. These differences are believed to be correlated with different modes of seed dispersal. The species also differ in ultimate fate of the apical cell (*ca*) of the proembryo, but neither taxonomical significance of this distinction nor its ecological importance are known.

Keywords: anther, development, embryo, embryology, funicle, ovule, pollen, seed, Portulacaceae, Talinaceae, *Talinum*

The genus *Talinum* Adans. includes ca. 50 species of semisucculent herbs or subshrubs distributed in the tropics and subtropics of America, Africa and Asia (Gusev 1980). This genus was traditionally regarded as a member of Portulacaceae (Pax 1889; Takhtajan 1987; etc.). Molecular phylogenetic data support the segregation of a separate family – Talinaceae – comprising the genera *Amphipetalum, Talinella, Talinum*, with restricting Portulaceae s.str. to the genus *Portulaca* only (Nyffeler & Eggli 2010).

Extensive comparative studies of Talinaceae and Portulacaceae are needed to find useful phylogenetic markers in the group. Embryology of some *Talinum* species has been studied previously (Guignard 1965; Nyananyo 1993; Nyananyo & Olowokudejo 1986) but many questions still remain unresolved. This study is aimed to fill some structural and developmental gaps in embryology of *Talinum*. For our investigation, we selected *T. triangulare* (Jack.) Willd. and *T. paniculatum* (Jacq.) Gaertn. because the former has been recognized as a type species of the genus *Talinum* (von Poellnitz 1934; McNeill 1977; Brummitt 1978; Ferguson 2001) and the latter better fits typical characteristics of the genus (see De Candolle 1828; Pax 1889; McNeill 1974; Bair et al. 2006).

Materials and Methods

Living plants of *T. paniculatum* and *T. triangulare* were received from Komarov Botanical Institute of Russian Academy of Sciences (St Petersburg) and from Tsytsyn Main Botanic Garden of Russian Academy of Sciences (Moscow). Plants were grown under laboratory conditions where they copiously flowered and successfully set viable seeds.

Talinum paniculatum has rather small pink flowers about 3 mm in diameter, whereas flowers of *T. triangulare* are white and up to 6 mm in diameter. Both species opened their flowers for 2–4 h in the middle of the day. After that, withering tepals became curved inwards and closely appressed to the ovary so that the stamens touched the stigma providing self-pollination.

For light microscope observations (LM), buds on different developmental stages, anthetic flowers and fruits were fixed in formalin acetic alcohol (FAA), transferred into 70% alcohol and embedded in paraffin. Embedded material was sectioned at 8–12 µm using standard methods of serial sectioning (e.g., Barykina et al. 2004). Serial transverse (TS) and longitudinal (LS) sections were stained in Rawitz Haematoxylin or Safranin and Light Green or Alcian Blue and mounted in Canadian Balm. Sections were also stained with a PAS (Periodic acid-Shiff) reaction to detect all carbohydrates (including starch grains) and with Procyonic Blue to detect proteins. To detect lipids, sections we stained with Sudan-IV using fresh material as described in Barykina et al.

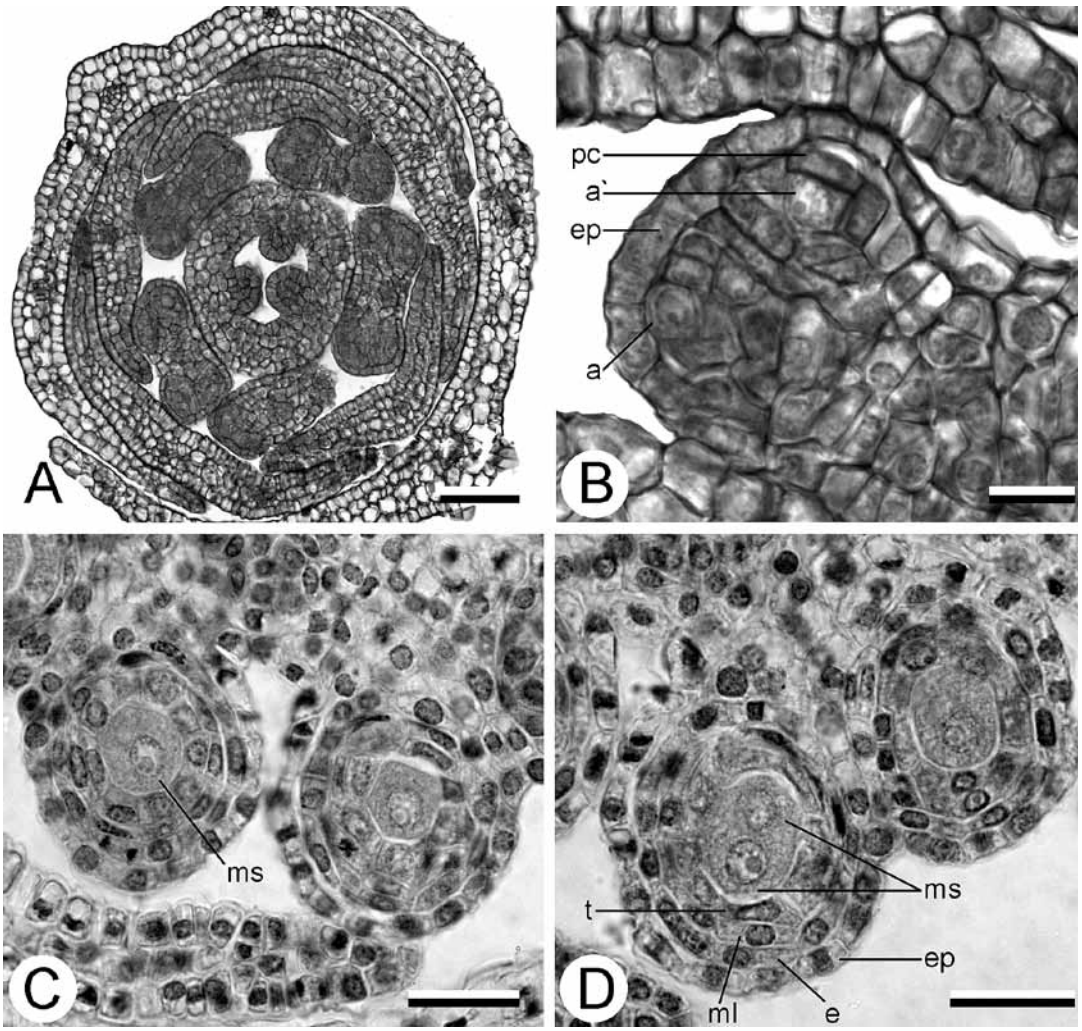

Figure 1. *T. paniculatum*, anther development (TS). A, B – archesporium formation. C, D – microsporocytes surrounded by four-layered anther wall. a – primary archesporium; a' – secondary archesporium (sporogenous cells); e – endothecium; ep – epiderm; ml – middle layer; ms – microsporocytes; pc – parietal cell; t – tapetum. Scale bars: in A = 50 µm; in B = 10 µm; in C–D = 20 µm.

(2004). Digital photomicrographs were made using a Zeiss Axioplan photomicroscope equipped with an AxioCam MR digital camera.

For scanning electron microscopy (SEM), dry intact seeds as well as dissected ones were mounted on stubs and then coated with gold and palladium using an Eiko IB-3 ion-coater (Tokyo, Japan). Observations were made using a CamScan S2 SEM (Oxford, UK) at the Laboratory of Scanning Electron Microscopy (Lomonosov Moscow State University). LM and SEM photos were processed and edited using Adobe Photoshop.

Results

In the terms of embryology, *T. paniculatum* and *T. triangulare* are very similar.

Anthers. The anthers are tetrasporangiate, dithecal. The anther wall develops centripetally following the monocot-type. The fully developed anther wall consists of epidermis, endothecium, middle layer and tapetum (Figs 1, 4). Epidermal cells in *T. triangulare* form bubble-like outgrowths whereas the epidermal cells in *T. paniculatum* remain flat (Fig. 5 C). Cells of the endothecium develop typical fibrous thickenings in their cell walls. The middle layer disintegrates when microsporocytes undergo meiosis (Fig. 2 B). The tapetum is of secretory type. Each of its cells has two to several nuclei that can fuse to produce a large multi-nucleolate cell (Fig. 2 D). The tapetum remains functional up to the stage of 2-celled pollen (Fig. 3 E–F). Crystals of calcium oxalate appear in cells of the connective and septa between theca locules. These crystals are larger in *T. triangulare* (Fig. 5 A, C). At anthesis, the mature anther wall is composed only by epidermis and fibrous endothecium, whereas the middle layer and tapetum completely disappear.

The sporogenous tissue is mostly uniseriate and consists of 5–8 cells in *T. paniculatum* and up to 10 cells in *T. triangulare* (Figs 2 A–B, 4 C), though the biseriate tissue is sometimes present in middle part of the anther (Fig. 2 C). Uniseriate and partly biseriate sporogenous tissue can be seen in different microsporangia of the same anther (Fig. 1 D). Meiosis results in formation of tetrahedral and isobilateral microspore tetrads covered by a thick callose sheath (Figs 3 A–C, 4 F).

The pollen grains are spherical, polyporate, ca. 57 μm in diameter in *T. triangulare* and spherical, polycolpate, about 46 μm in diameter in *T. paniculatum*. In both species, pollen grains are 3-celled, with well-visible cytoplasm of the two sperm cells (Figs 5–6). The pollen grains contain starch, proteins and lipids. Pollen fertility is close to 100%.

Anthers dehisce shortly before flower opening, so that the just opened flowers already have some released pollen grains attached to their stigmas. Dehiscence of the anther is likely to be resulted from high tension of its wall, because the latter curves inside out to expose the fibrous layer after the anther has dehisced (Fig. 5 D). When the flower closes again, the withering tepals push the anthers to contact the stigma to ensure self-pollination.

Gynoecium. The gynoecium is syncarpous and typically consists of three carpels, though *T. paniculatum* occasionally has a 2- or 4-merous gynoecium. The placentation is axile in the young buds. However, septae between ovary locules disappear resulting in a columnar placentation in the older buds at the stage of megasporocyte formation.

Each carpel consists of fertile ascidiate and sterile plicate zones. *T. paniculatum* usually develops 15–20 ovules per ovary, whereas *T. triangulare* develops 25–65 ovules. All ovules are attached to the placenta in the synascidiate zone, but they are lifted upwards by their funicles into the

symplicate zone. The ovules are anacampylotropous, crassinucellate, bitegmic and endostomous (i.e. with a micropyle formed by the inner integument). Both integuments are mostly 2-layered, though the number of cell layers is slightly greater in the micropyle region. There is a narrow space between the integuments in the chalazal region (Fig. 8 E).

Nucellus. The nucellus develops a single archesporial cell in both species. This cell periclinally divides to produce outwards a parietal cell which in turn divides 1(2) time(s) to give rise to the parietal layer (Figs 7 A–C, 10 A). During megasporogenesis and early stages of embryo sac development, this feeble parietal layer degenerates as well as the nucellus cells which adjoin the progressing embryo sac. Simultaneously, the epidermal cells of the nucellus located nearby the micropyle divide periclinally to form a nucellar cap. The latter consists of about four cell layers

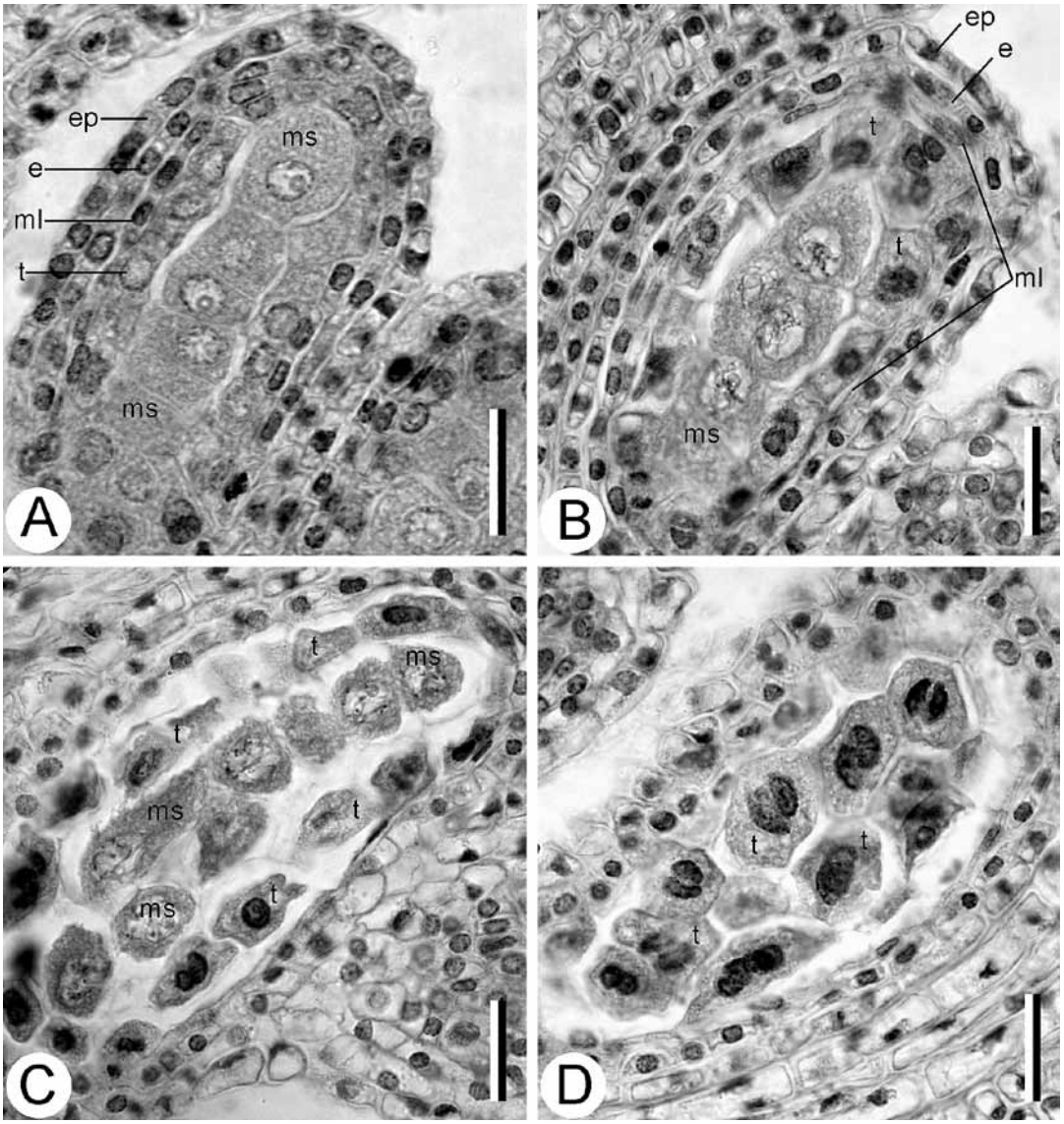

Figure 2. *T. paniculatum*, microsporogenesis (LS). A – uniseriate archesporium. B, C – archesporial cells partly in two rows. D – tapetum. e – endothecium; ep – epiderm; ml – middle layer; ms – microsporocytes; t – tapetum. Scale bars = 20 µm.

and touches the embryo sac up to a half of its length (Fig. 9C). The epidermal cells of the nucellus located just below the micropyle divide only once or do not undergo divisions at all. Instead, they increase their length in longitudinal direction. These long cells eventually facilitate pollen tube growth through the nucellus (Fig. 8A). Thick pollen tubes remain during the proembryo development.

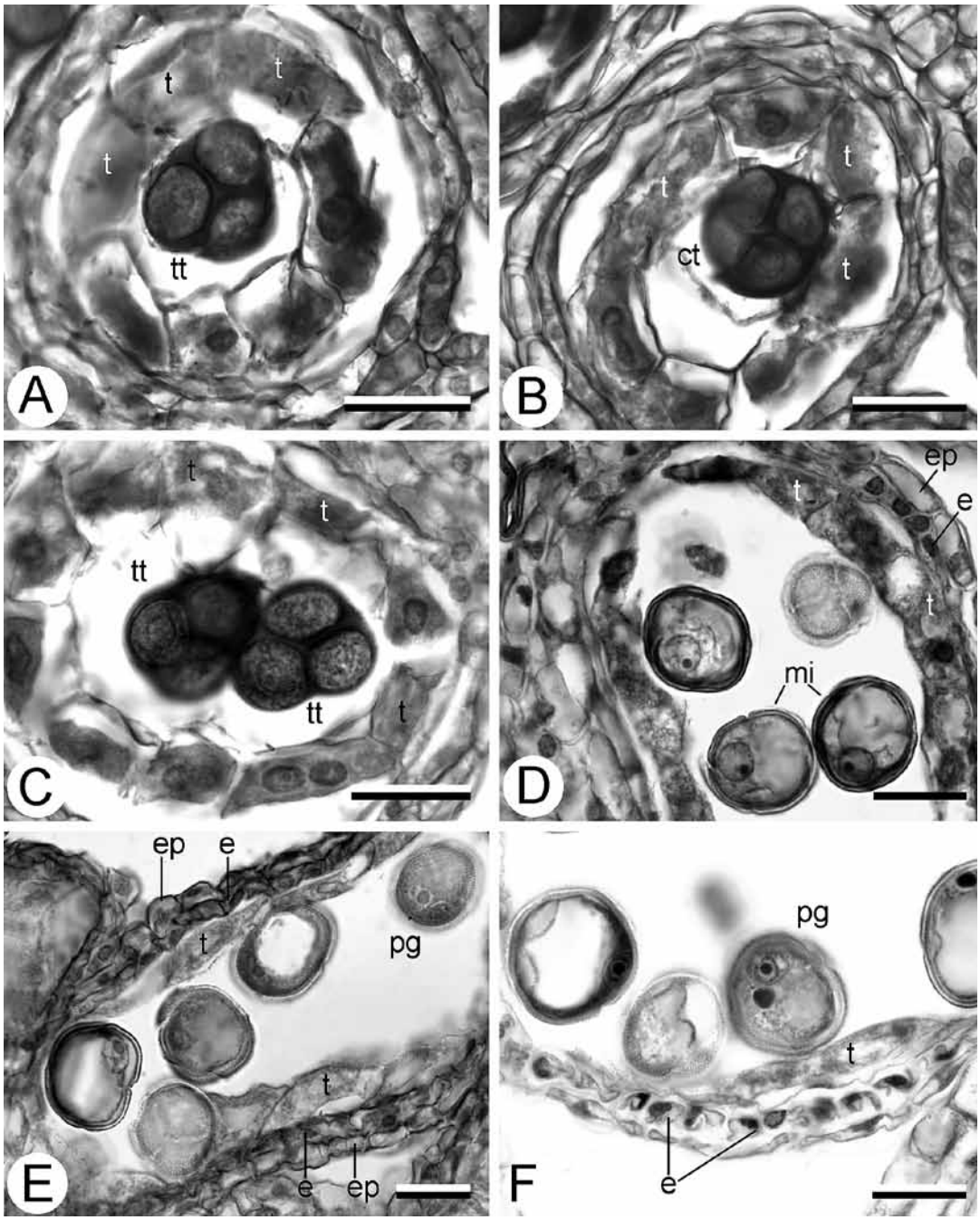

Figure 3. *T. paniculatum*, pollen development (TS). A, B, C – microspore tetrads. D – microspores at late post-tetrad period. E, F – two-celled pollen grains. ct – cross tetrad; e – endothecium; ep – epiderm; mi – microspore; pg – pollen grain; t – tapetum; tt – tetrahedral tetrad. Scale bars = 20 µm.

Megasporogenesis. In both species examined, cell divisions of the micropylar cell of the dyad are characteristically suppressed. This results in a triad of cells instead of a tetrad. Micropylar cell of the dyad degenerates, whereas the chalazal one produces two megaspores (Figs 7 E–F, 10 B). The chalazal megaspore gives rise to the embryo sac.

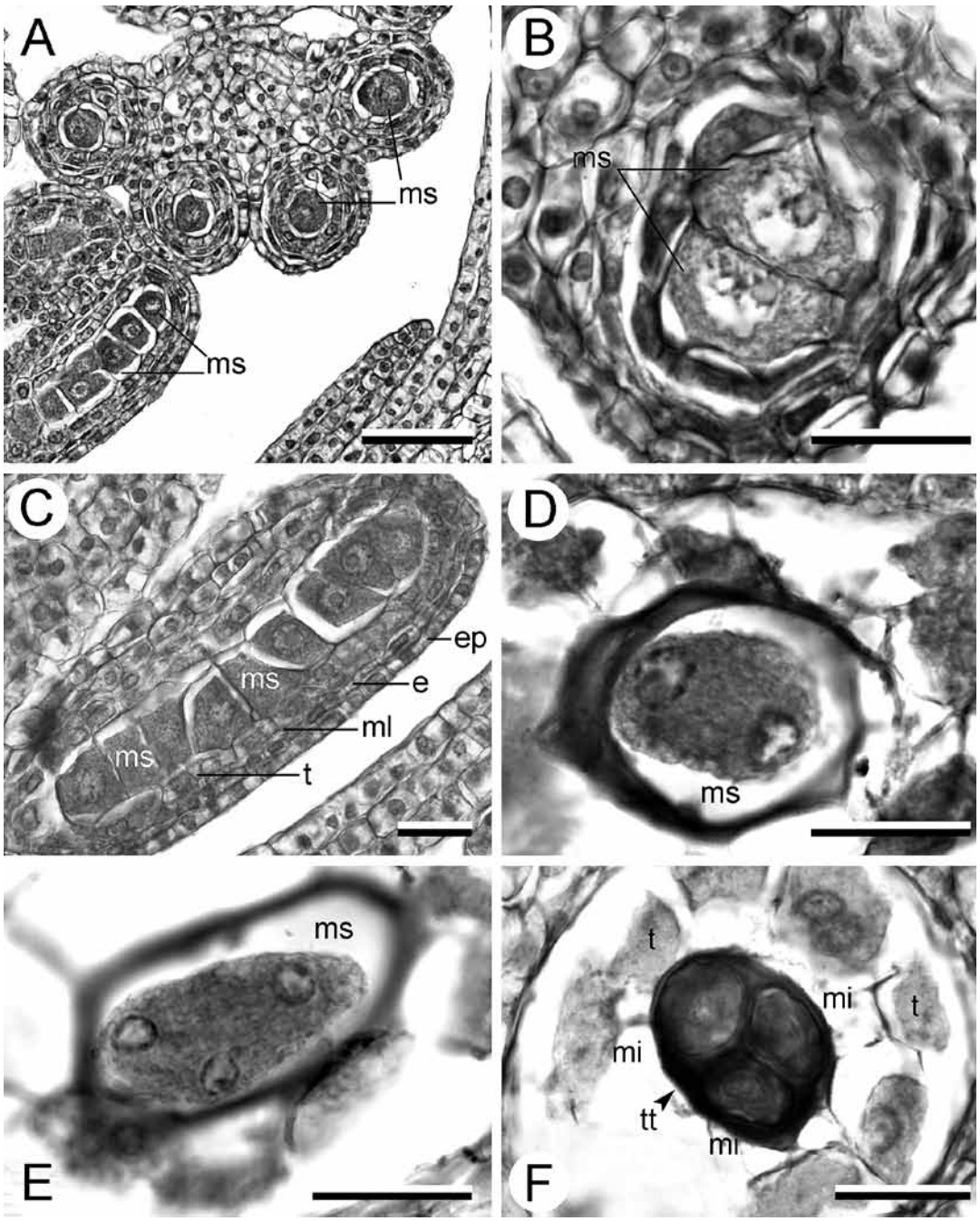

Figure 4. *T. triangulare*, microsporogenesis (TS and LS). A – microsporocytes (TS, LS). B – two microsporocytes (TS). C – uniseriate archesporium (LS). D, E – meiosis (TS). F – microspores in tetrahedral tetrad (TS). e – endothecium; ep – epiderm; mi – microspore; ml – middle layer; ms – microsporocytes; t – tapetum; tt – tetrahedral tetrad. Scale bars: in A = 50 μm; in B–F = 20 μm.

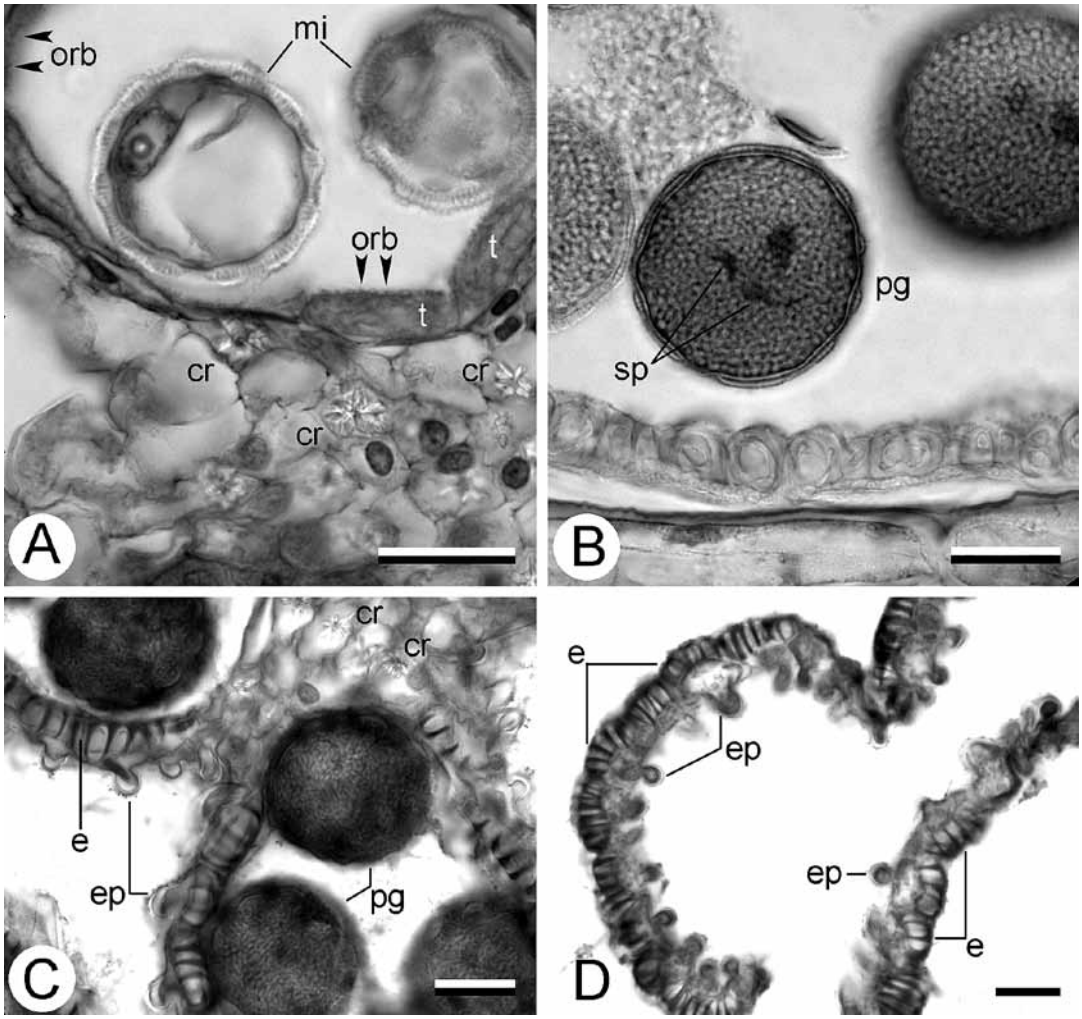

Figure 5. *T. triangulare*, pollen development (TS). A – microspores at late post-tetrad period. B, C – three-celled pollen grains. D – dehisced anther. cr – calcium oxalate crystals, e – endothecium; ep – epiderm; mi – microspore; orb – orbicules (Ubish bodies) on tapetal cells; pg – pollen grain; sp – sperm cells; t – tapetum. Scale bars = 20 µm.

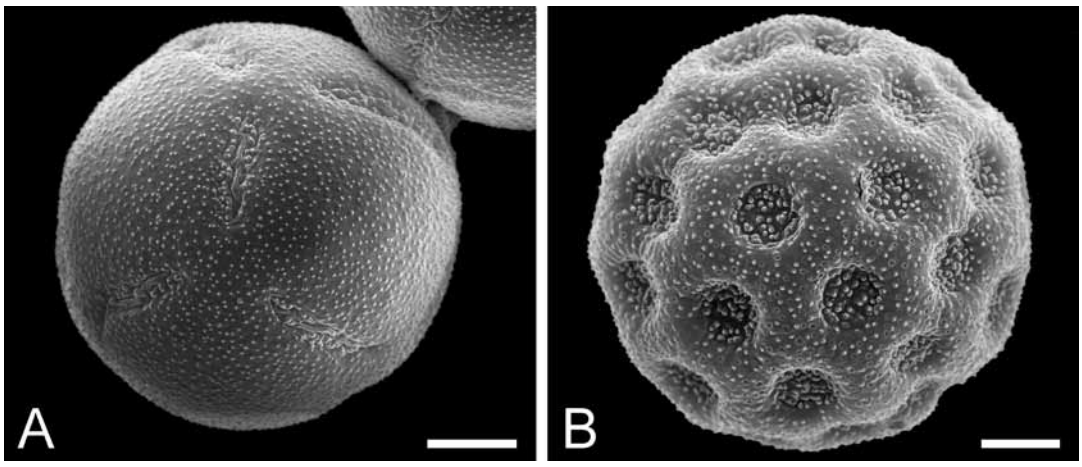

Figure 6. Mature pollen (SEM). A – *T. paniculatum*. B – *T. triangulare*. Scale bars = 10 µm.

Embryo sac. The embryo sac is of Polygonum-type (Fig. 8) and has an egg apparatus of typical structure (Figs 9, 10 E–F). The synergids bear hook-like outgrowths and a filiform apparatus. The egg cell contains starch grains. The polar nuclei of the primary endosperm fuse before fertilization. The resultant secondary nucleus is surrounded by numerous starch grains. The ephemeral antipodals are usually absent in the mature embryo sac.

Funicle. The funicle of *T. triangulare* is longer than that in *T. paniculatum*. In both species, the distalmost part of the funicle adjacent to the ovule changes characteristically during seed development. It develops a parenchymatous outgrowth in counter direction of the micropyle (Fig. 11 A–C). This outgrowth further differentiates into an aril. In *T. triangulare*, the parenchyma cells of the protruding part of the aril are larger than the others (Fig. 11 G). In *T. paniculatum*, all cells of the aril are uniform (Fig. 11 C). They are generally smaller than those of *T. triangulare*. In funicles of both species, a small-celled abscission zone develops below the aril prior to seed releasing. The lower part of the funicle remains attached to the placenta after the seeds have been shed off (Fig. 11 D–E, I).

The funicle transformation is more complicated in *T. paniculatum*, whose funicle epidermal cells located below the presumptive aril enlarge and detach from the inner tissue prior to fertilization

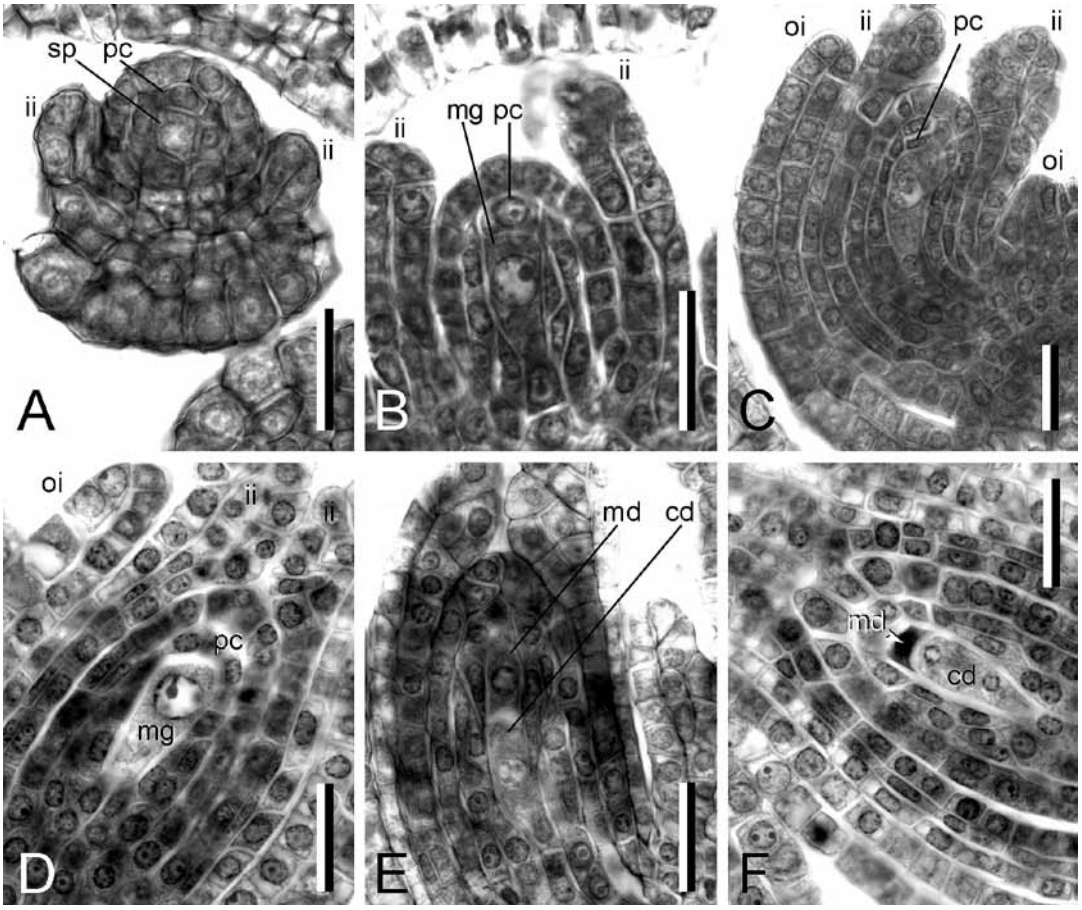

Figure 7. *T. paniculatum*, megasporogenesis (LS). A – sporogenous and parietal cells. B–D – megasporocyte (megaspore mother cell). E – dyad. F – mitosis in dyad chalazal cell. cd – dyad chalazal cell; ii – inner integument; mg – megasporocyte; md – dyad micropylar cell; oi – outer integument; pc – parietal cell; sp – sporogenous cell. Scale bars = 20 µm.

to form a sheath around the inner solid part of the funicle (Fig. 11 A). This detached epidermis consists of large spherical cells with thin unlignified cell walls with fibrous cell wall thickenings resembling those of anther endothecium. Their protoplasts contain elaioplasts (Fig. 11 C, F). The entire structure remains attached after seed releasing (Fig. 11 D–E). Apparently, these transformed funicle remnants have been mistaken with underdeveloped ovules by Galati (1986).

Aril. The aril of the mature seed of *T. paniculatum* is a small white plicate body whose cells contain neither reserve lipids, nor proteins, nor starch. The aril of the mature seed of *T. triangulare* is larger than that of *T. paniculatum*. It has smooth surface and consists of large thin-walled cells with well-visible nuclei and dense cytoplasm containing both lipids and proteins in large quantities (Fig. 11 H). In dried seeds, the arils of both species look similar, especially in SEM (Fig. 19 A, D).

Embryo development. The embryo development was scrutinized in *T. triangulare*. 24 h after pollination, the zygote slightly elongates longitudinally and then divides transversally to give rise to a 2-celled proembryo which is composed of a small apical cell (*ca*) with dense cytoplasm and a

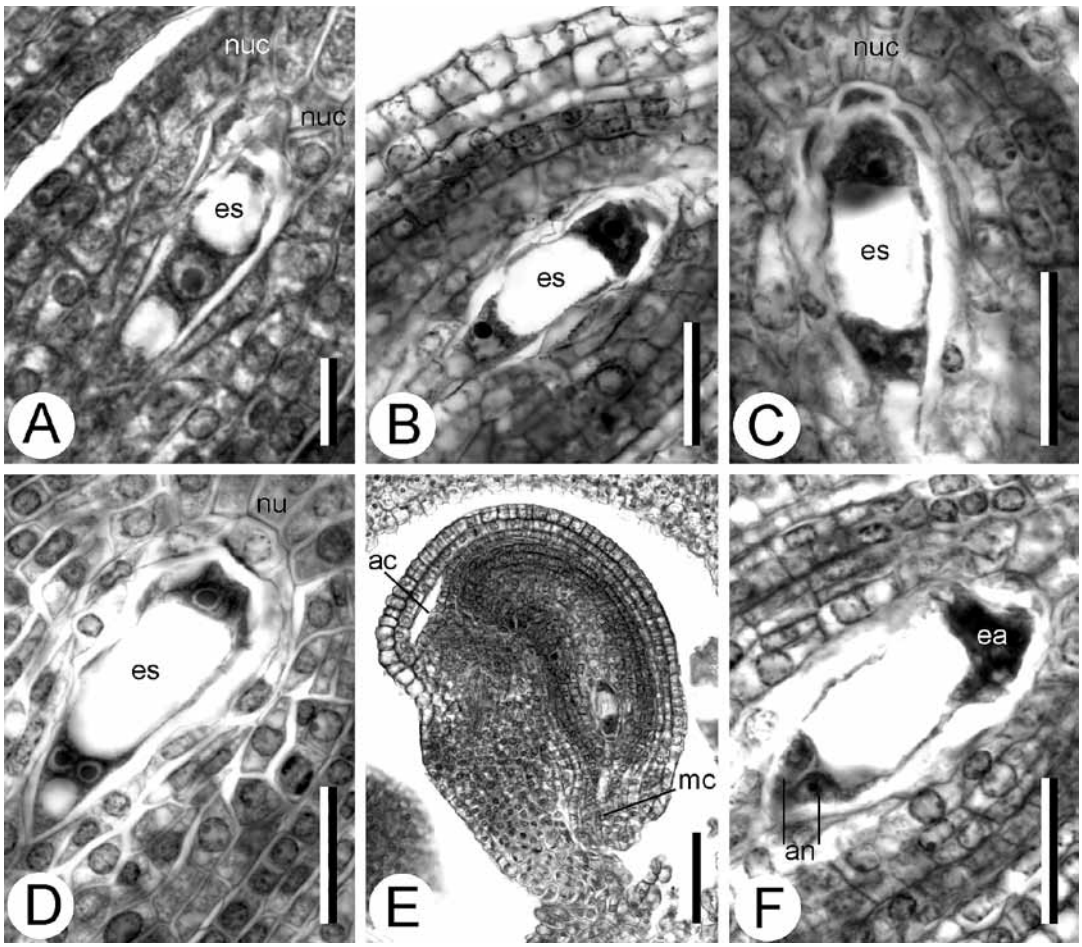

Figure 8. *T. paniculatum*, embryo sac development (LS). A– 1-nucleate embryo sac. B – 2-nucleate embryo sac. C, D – 4-nucleate embryo sac. E – immature embryo sac inside young ovule. F – 8-nucleate embryo sac with antipodals and egg apparatus. an – antipodals; ac – air cavity; ea – egg apparatus; es – embryo sac; mc – micropyle; nu – nucellus; nuc – nucellar cap. Scale bars: in A = 10 µm; in B–D, F = 20 µm; in E = 50 µm.

larger basal cell (*cb*) with a large vacuole (Fig. 12 A–B). Then, both cells also divide transversely yielding a linear 4-celled proembryo (Fig. 12 C). The cell *ca* produces a basal cell *l'* and a distal cell *l*. The cell *cb* gives rise to the basal cell *ci* and distal cell *m*. The cells *l* and *m* are smaller and have denser cytoplasm than their sister cells *l'* and *ci*, respectively. The proembryo cells *l* and *l'* (derivatives of *ca*) both divide longitudinally (the possibility that *l* divides either prior or after *l'* is equal). Simultaneously (or even before that), the transverse division of the basal proembryo cell *ci* (which is a derivative of *cb*) takes place (Fig. 13 A–D). Division of the cell *m* (which is a distal derivative of *cb*) is slightly delayed. It divides only after the 2–3-celled suspensor has been formed as a result of divisions of *ci* and mostly after 1–2 divisions of the two distal cells have taken place (Fig. 13 C, E). Its distal daughter cell *m'* represents a presumptive hypophysis of globular embryo. It further divides longitudinally (Fig. 14 A–C). The basal daughter cell *n* and its derivatives evolved from several transversal and longitudinal cell divisions form the distal part of the multicellular suspensor (Fig. 14 B–D). The basalmost massive part of the latter directly originates from the basalmost cell *ci* of the 4-celled proembryo. It forms an anchor-shaped

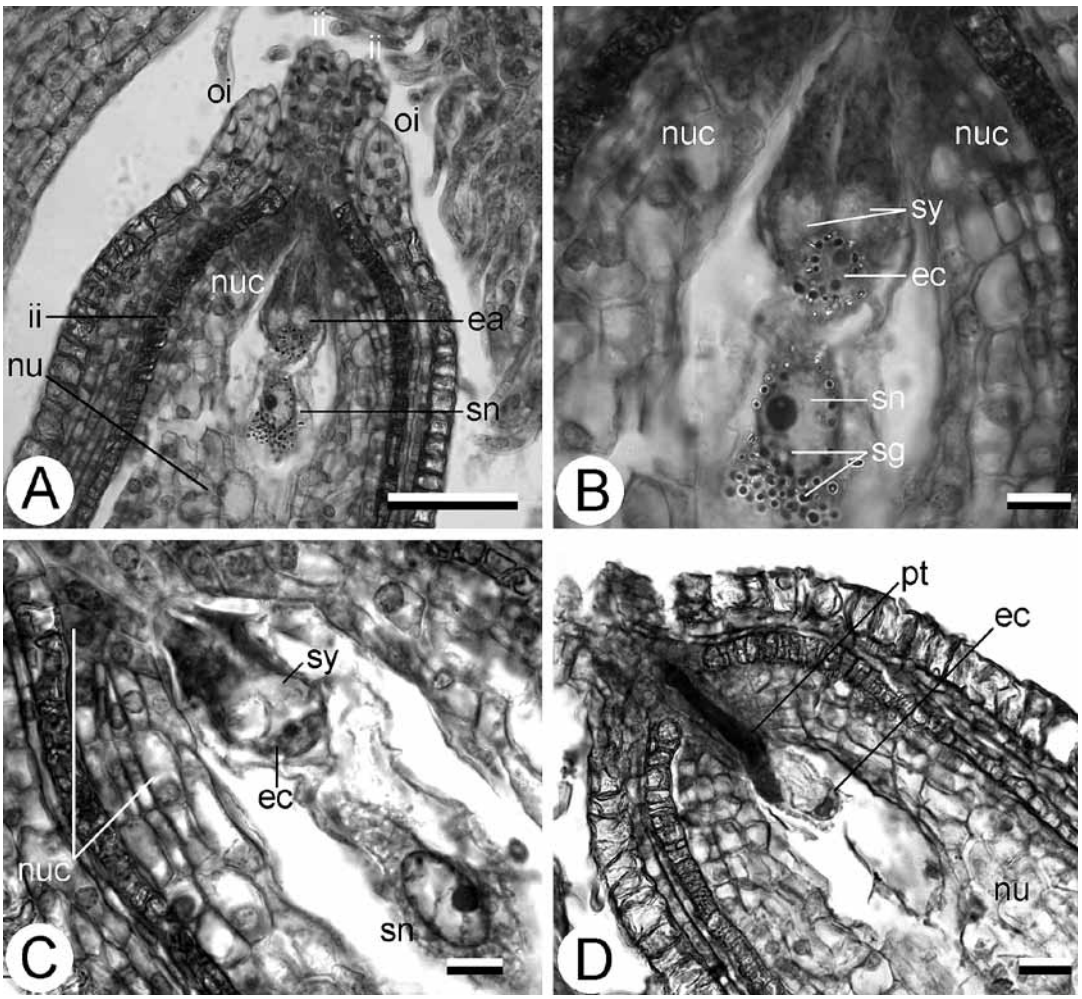

Figure 9. *T. paniculatum*, mature embryo sac (LS). A–D – egg apparatus. ea – egg apparatus; ec – egg cell; ii – inner integument; nu – nucellus; nuc – nucellar cap; pt – pollen tube; sg – starch grains; sn – secondary nucleus; sy – synergids. Scale bars: in A = 50 µm; in B–C = 10 µm; in D = 20 µm.

support which tightly touches the nucellus (Fig. 14C,–D). The embryo *per se* is formed by *l* and *l'* layers (derivatives of the cell *ca*). Thus, the embryo development of *T. triangulare* follows Solanad-type.

Talinum paniculatum also develops a 4-celled proembryo (Fig. 15B–C, E). First cell divisions of its two distal cell layers are apparently longitudinal as in *T. triangulare* (Fig. 15F). The hypophysis and the small suspensor are formed at the stage of late globular embryo. The suspensor is distally uniseriate and basally few-seriate, so it is less developed than its counterpart in *T. triangulare* (Fig. 15G–H). The embryo *per se* is formed by both derivatives of the cell *ca* (Fig. 15F–G) and thus corresponds to Solanad-type just as in *T. triangulare*.

Endosperm development. The endosperm is of nuclear type. Its cellularization commences at its micropylar end simultaneously with the initiation of embryo cotyledons (Figs 14D, 16A). Endosperm cells contain small starch grains and protein inclusions. Thereof, the reserve substances of the endosperm are soluble. The chalazal end of the endosperm differentiates into massive

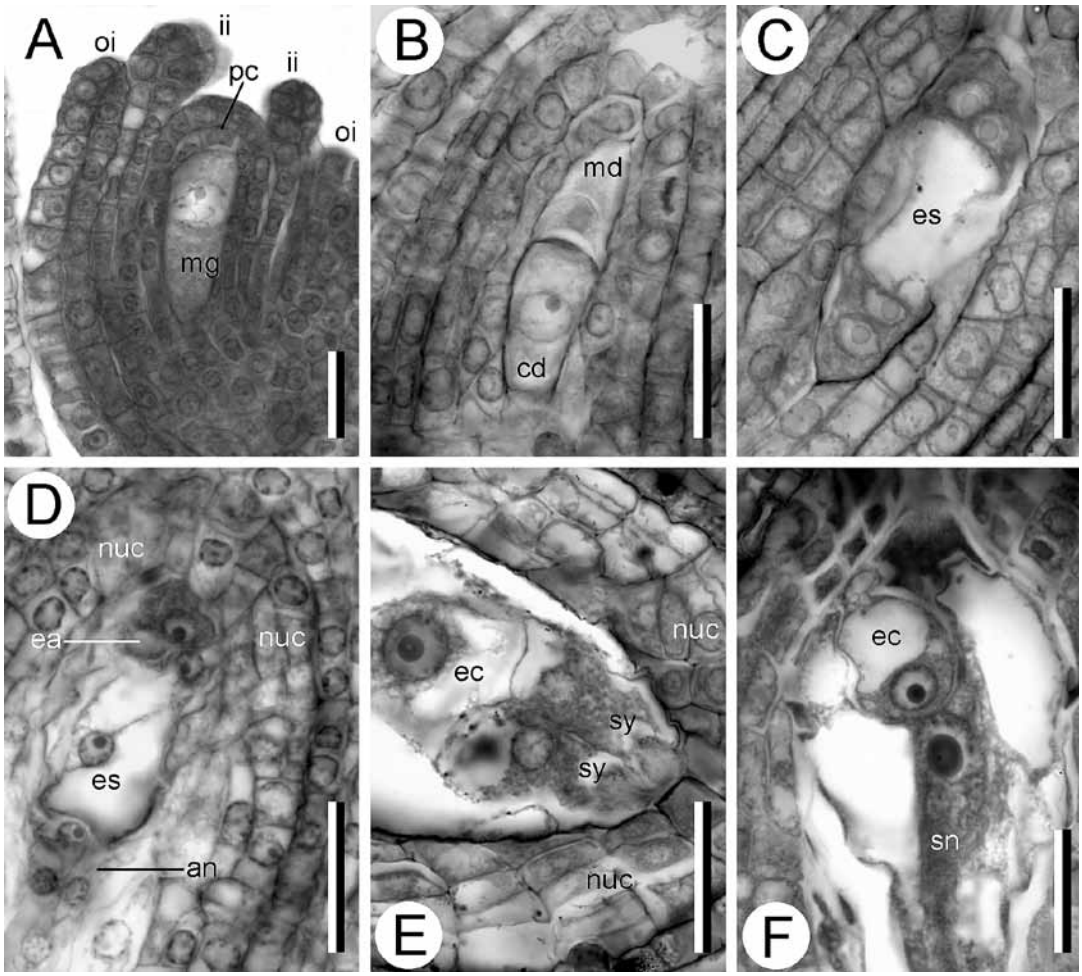

Figure 10. *T. triangulare*, megasporogenesis and embryo sac development (LS). A – megasporocyte. B – dyad. C – 4-nucleate embryo sac. D – 8-nucleate embryo sac. E, F – mature embryo sac, micropylar end. an – antipodals; ea – egg apparatus; ec – egg cell; cd – dyad chalazal cell; ii – inner integument; md – dyad micropylar cell; mg – megasporocyte; nuc – nucellar cap; oi – outer integument; pc – parietal cell; sn – secondary nucleus; sy – synergids. Scale bars = 20 μm.

haustorium at the early stages of embryo development. It is represented by dense cytoplasm containing large nuclei and rod-like protein bodies (Figs 16 A–B, 17 E). The haustorium extends to the seed vascular bundle. At this stage, nucellar cells surrounding the haustorium contain extensive starch deposits (Fig. 17 B). The wall of endospermal haustorium contacting the nucellus is thickened and resembles those of transfer cells (Fig. 17 C–F). The part of the haustorium that faces the nuclear endosperm develops transparent bubble-like protuberances with small protein grains on their surfaces, which jut into the endosperm (Fig. 17 C–D, F). At later stages of seed development, haustorial activity gradually ceases and haustorial nuclei and cytoplasm collapse into a homogeneous mass, which is further demolished by the developing embryo. The cotyledon tips are situated on the place of former haustorium in the mature seed.

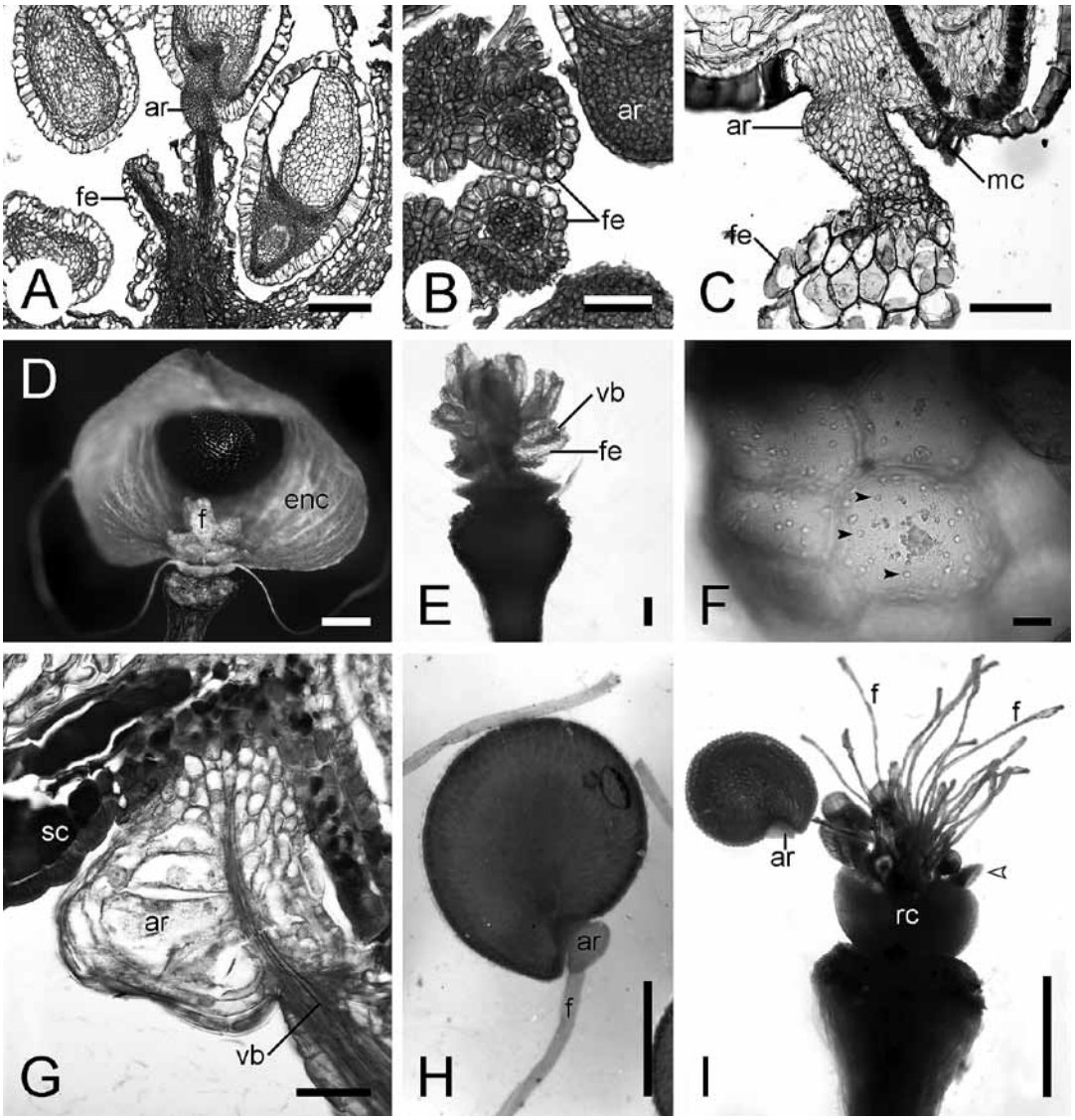

Figure 11. Arils and funicles. A–F – *T. paniculatum*. G–I – *T. triangulare*. ar – aril; enc – endocarp; f – funicle; fe – funicular epiderm; mc – micropyle; rc – receptacle; sc – seed coat; vb – vascular bundle. Black arrowheads indicate lipid drops. White arrowhead indicates sterile ovule. Scale bars: in A, D–E = 200 μm; in B–C = 100 μm; in F = 20 μm; in G = 50 μm; in H = 500 μm; in I = 1 mm.

Seed interior development. Soon after fertilization, the anacampylotropous ovule changes into an amphitropous one due to the intensive growth in its chalazal region. Both micropyle and chalazal part are situated at the same level at the stage of proembryo (Fig. 15 A). The curving of the nucellus is followed by the curving of the embryo sac.

In the mature seed, the endosperm is almost entirely consumed by the embryo and is represented by protein-rich cap cells that cover the tip of the primary root (Fig. 16 E). The coiled embryo surrounds the perisperm, whose cells contain densely packed starch grains. The cells of the fully developed embryo contain copious aleuron grains and lipid drops but do not have starch (Fig. 16 E–G). Starch grains are discernible only in the root cap of the primary root where they will act as statoliths after seed germination (Fig. 14 F).

Seed coat development. The seed coat is formed by both integuments in both *T. paniculatum* and *T. triangulare*. The cells of the outer layer of the outer integument and those of the inner

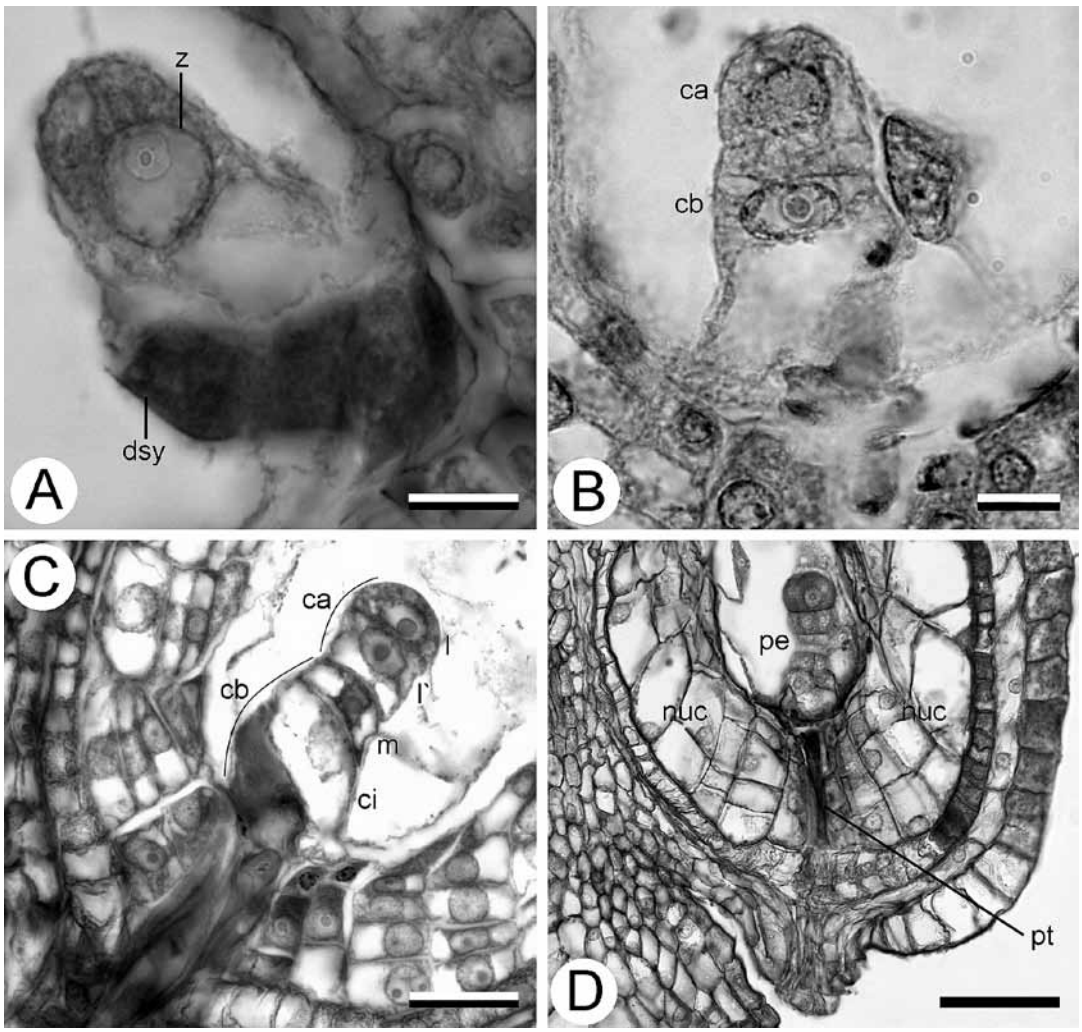

Figure 12. *T. triangulare*, proembryo development (LS). A – zygote. B – two-celled proembryo. C – four-celled proembryo. D – micropylar region of an ovule with proembryo. ca – apical cell of two-celled proembryo; cb – basal cell of two-celled proembryo; dsy – degenerating synergid; l and l' – derivates of ca; ci and m – derivates of cb; nuc – nucellar cap; pe – proembryo; pt – pollen tube. Scale bars: in A–B = 10 µm; in C = 20 µm; in D = 50 µm.

layer of the inner integument enlarge immediately after germination. They accumulate tannins in their vacuoles at first as numerous yellowish-brown small grains and then as large ones that further amalgamate (Fig. 18 A–E). These cells also accumulate proteins and carbohydrates. The inner layer of the outer integument and the outer layer of the inner integument contain starch grains at the early stages of seed development. These layers become empty and obliterated soon afterwards. The cells of the inner layer of the inner integument gradually lose their protoplasm. Thereof, this layer consists of thin-walled empty cells in the mature seed. This layer is referred to as endotegmen (Fig. 18 C–E). The endotegmic cells are characterized by parallel secondary cell-wall thickenings appearing as radial striation (Fig. 19 C, F).

The seed coat mainly comes from the outer epidermis of the outer integument. It is thus an exotesta. The exotestal cells accumulate tannins and develop thickened outer walls penetrated by numerous pore canals (Figs 18 C–E, 19 B, E). These canals make a reticulate pattern on the cell

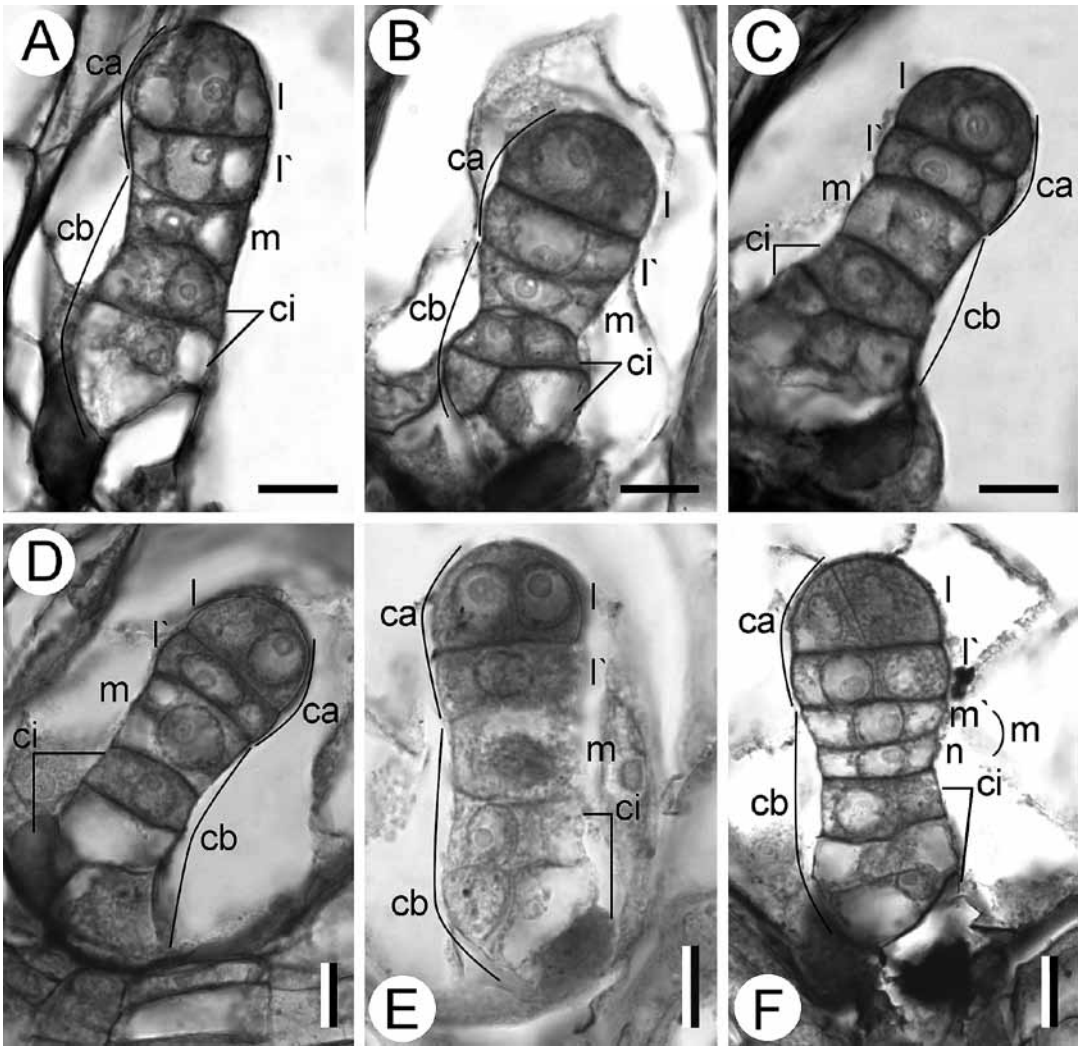

Figure 13. *T. triangulare*, proembryo. A–F – development, continuation. (LS). ca – derivates of apical cell of two-celled proembryo; cb – derivates of basal cell of two-celled proembryo; l and l' – derivates of ca; ci and m – derivates of cb; n and m' – derivates of m. Scale bars = 10 μm.

surface (Fig. 18 F). Impregnated by deep-brown tannins and covered by thick cuticle, the outer cell wall is the most prominent part of each exotestal cell in the mature seed (Fig. 19 B, E). The exotestal cell lumen is reduced to a narrow slit. Thus, the seed coat of both species examined is of exotestal-endotegmic type.

Seed sculpture. Despite similarities in structure and development, the species examined differ in shapes and sizes of their exotestal cells and seed fine sculpture.

Seeds of *T. paniculatum* are almost black, glossy, ca. 1 mm long, reniform, laterally compressed. Their micropylar end is slightly protruding the chalazal side. There is a depression (hilum area) between micropylar and chalazal ends where hilum and aril are located (Fig. 19 A). Under the light microscope, the exotestal cells are tetra- to hexagonal and slightly elongated towards the ventral side of the seed (Fig. 18 F). Their anticlinal cell walls are straight or slightly undulate, non-protruding the seed surface. In SEM, the seed surface is almost smooth, the outer cell walls are plane but there are deep cuticle depressions at places where three adjacent cells touch each other. The cells are more convex on the ventral side of the seed.

Seeds of *T. triangulare* are of same shape and colour as those of *T. paniculatum*, but slightly smaller. The exotestal cells are convex (especially in the hilum area), penta- to hexagonal. They

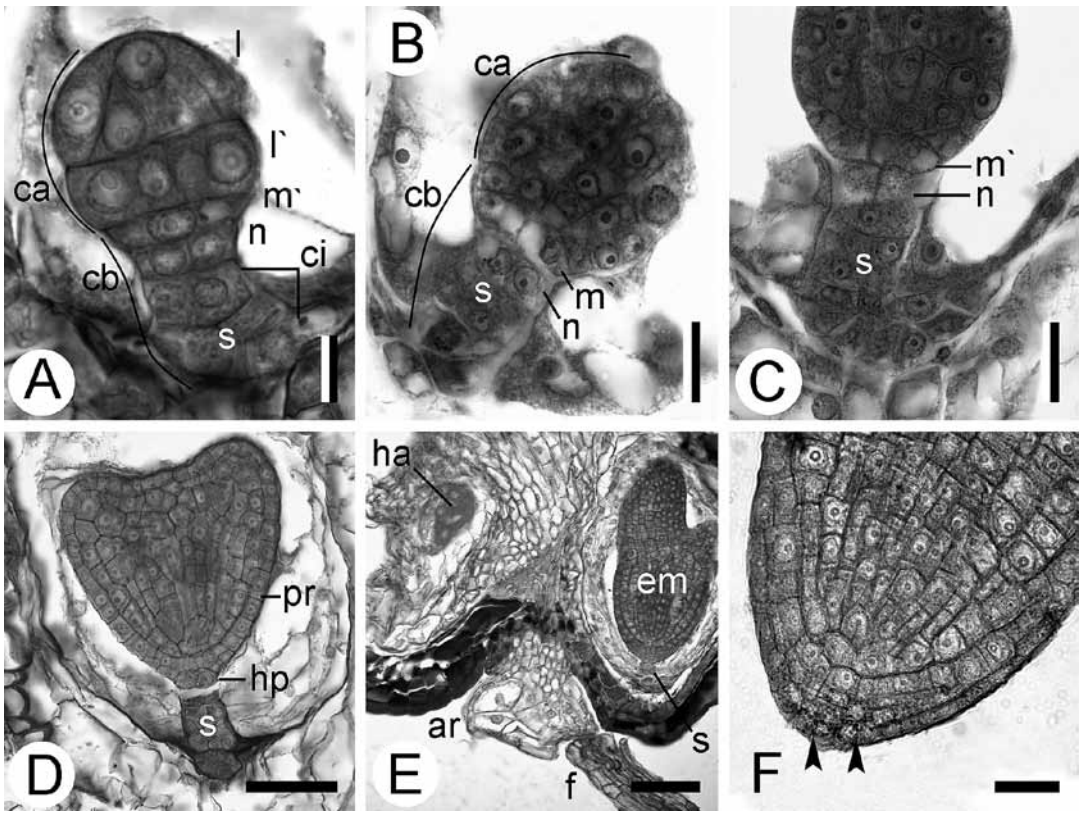

Figure 14. *T. triangulare*, embryo development (LS). A–C – globular embryo. D, E – development of cotyledons. F – apex of primary root with starch grains (statoliths) in the root cap. ar – aril; ca – derivates of apical cell of two-celled proembryo; cb – derivates of basal cell of two-celled proembryo; f – funicle; ha – endospermal haustorium; hp – hypophysis; l and l' – derivates of ca; ci, m' and n – derivates of cb (n, m' – derivates of m); pr – protoderm; s – suspensor. Black arrowheads show statoliths. Scale bars: in A = 10 µm; in B–C, F = 20 µm; in D = 50 µm; in E = 100 µm.

are slightly elongated on the lateral sides and almost isodiametric and in regular rows on the dorsal side of the seed. Their anticlinal cell walls are straight. Each cell in the hilum area has a papilla in central part of its outer cell wall (Fig. 19 D). There are special cells with oval orifice surrounded by a rim in hilum depression (Fig. 19 D).

Discussion

The species examined show embryological characters that are common for the majority of Centrospermae (= core Caryophyllales sensu APG III 2009). These are campylotropous bitegmic endostomous ovules, basal slit between the two integuments, ephemeral antipodals, presence of perisperm, coiled embryo, exotestal-endotegmic seed coat, longitudinal striation of tegmic cell walls, 3-celled pollen etc. At the same time, species of *Talinum* demonstrate characters which

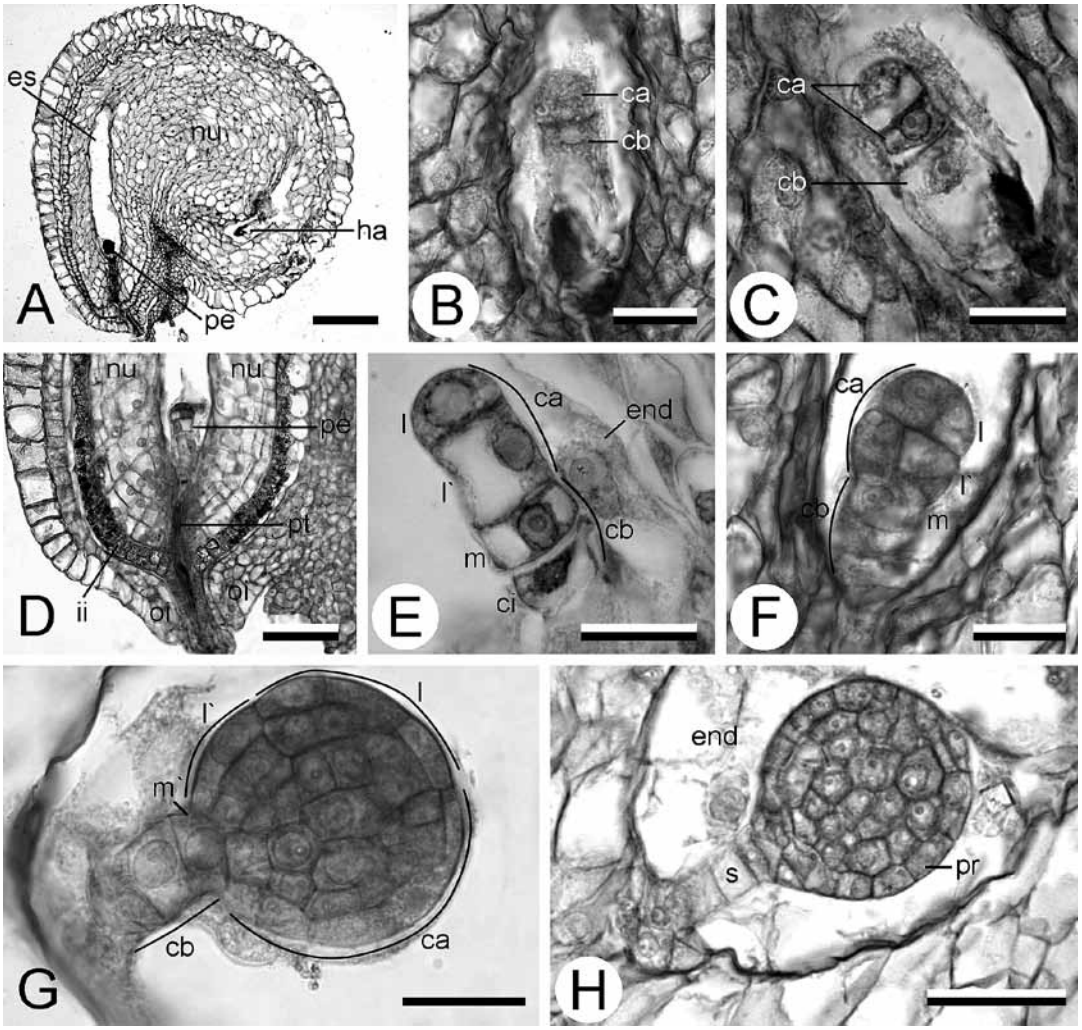

Figure 15. *T. paniculatum*, embryo development (LS). A – ovule with proembryo. B – two-celled proembryo. C – three-celled proembryo. D, E – four-celled proembryo. F – multicelled proembryo. G, H – globular embryo. ca –apical cell of two-celled proembryo and its derivates; cb –basal cell of two-celled proembryo and its derivates; end – endosperm; ha – endospermal haustorium, ii – inner integument; l and l' – derivates of ca; ci, m and m' – derivates of cb; m' – derivate of m; oi – outer integument; nu – nucellus; pe – proembryo; pr – protoderm; s – suspensor. Black arrowheads show statoliths. Scale bars: in A = 200 µm; in B–C, E–H = 20 µm; in D = 50 µm.

are rare for angiosperms, like anther archesporial cells arranged in a single row. Sometimes we also observed partly biseriate archesporial cells. Uniseriate archesporium of anther is a specific character of all members of Portulacaceae s.l. studied so far (Batygina 1983). Both *Talinum* and *Portulaca* demonstrate a 4-celled linear proembryo, an endospermal haustorium and thick

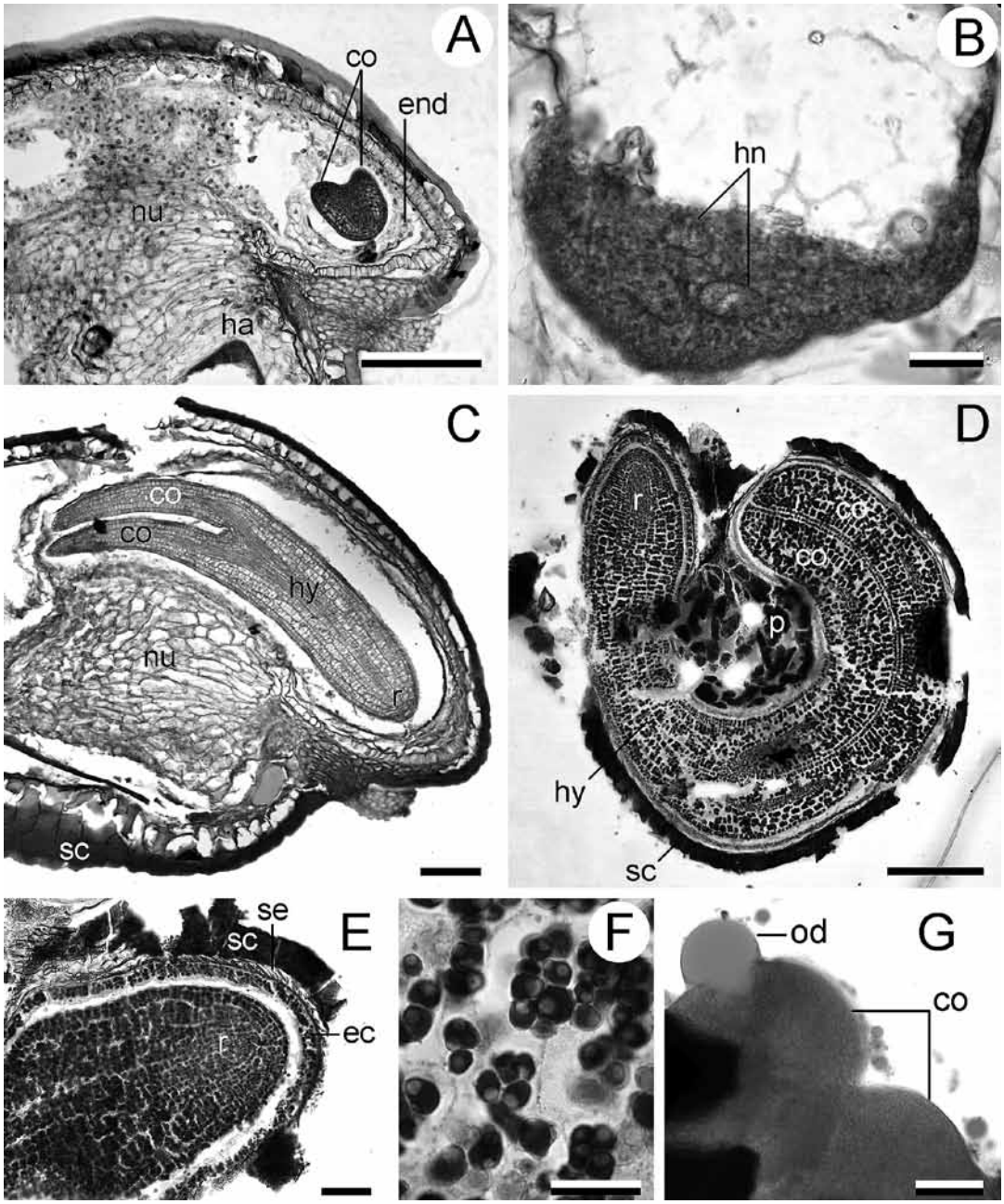

Figure 16. *T. paniculatum*, seed development (LS). A – micropylar end of an ovule with bilobed embryo. B – endospermal haustorium in immature seed. C – immature seed. D – mature seed. E – primary root in mature seed. F – aleuron grains in embryo cells. G – oil drops in squashed embryo. co – cotyledon; ec – endospermal cap; end – endosperm; ha – endospermal haustorium; hn – haustorial nuclei; hy – hypocotyl; nu – nucellus; od – oil drop; p – perisperm; r – primary root; sc – seed coat. Scale bars: in A, D = 200 µm; in B, F = 20 µm; in C, G = 100 µm; in E = 50 µm.

pollen tubes that remain long after the fertilization. Both species examined in the present study show Solanad-type of embryo development. The same type of embryo development has been found in *Portulaca oleracea* L. (Cooper 1940). Thus, embryological characters that are believed to be of taxonomical importance do not provide further support for recognizing a separate family Talinaceae.

Members of Portulacaceae s.l. in general demonstrate a high variability of seed coat anatomy (Plisko 1991), but *T. paniculatum* and *T. triangulare* are quite similar to *Portulaca* in the structure

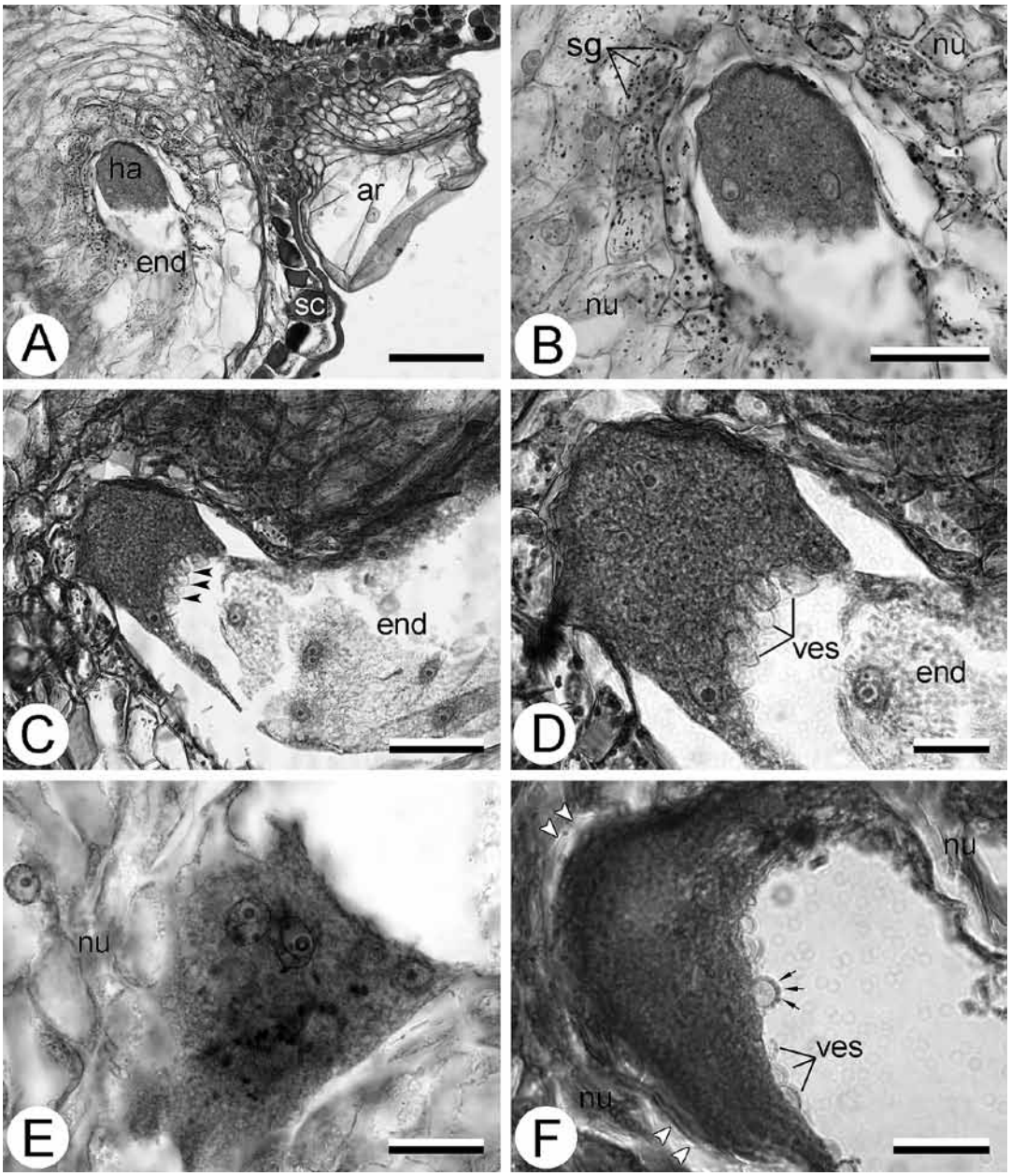

Figure 17. *T. triangulare*. A–F – endospermal haustorium (LS). ar – aril; end – endosperm; ha – endospermal haustorium; nu – nucellus; sc – seed coat; sg – starch grains; ves – vesicles. Black and white arrowheads indicate haustorial wall. Arrows indicate protein corpuscles on a vesicle. Scale bars: in A–C = 50 µm; in D–F = 20 µm.

of the exotesta. *Talinum* exotesta resembles that of *Pereskia* (see Vishenskaya 1991), the primitive member of Cactaceae, the latter being hardly discernible from Portulacaceae s. str. (Nyffeler & Eggli 2010). However, the exotesta of the investigated species is also similar to that of *Claytonia virginica* L. (former Portulacaceae; see Plisko 1991) which is now placed in the family Montiaceae (Stevens 2008; Nyffeler & Eggli 2010) and to the exotesta of *Pleuropetalum* (Amaranthaceae) (see Veselova & Timonin 2009). Thus, the seed coat structure plainly confirms neither a segregation of the family Talinaceae nor its inclusion into the family Portulacaceae.

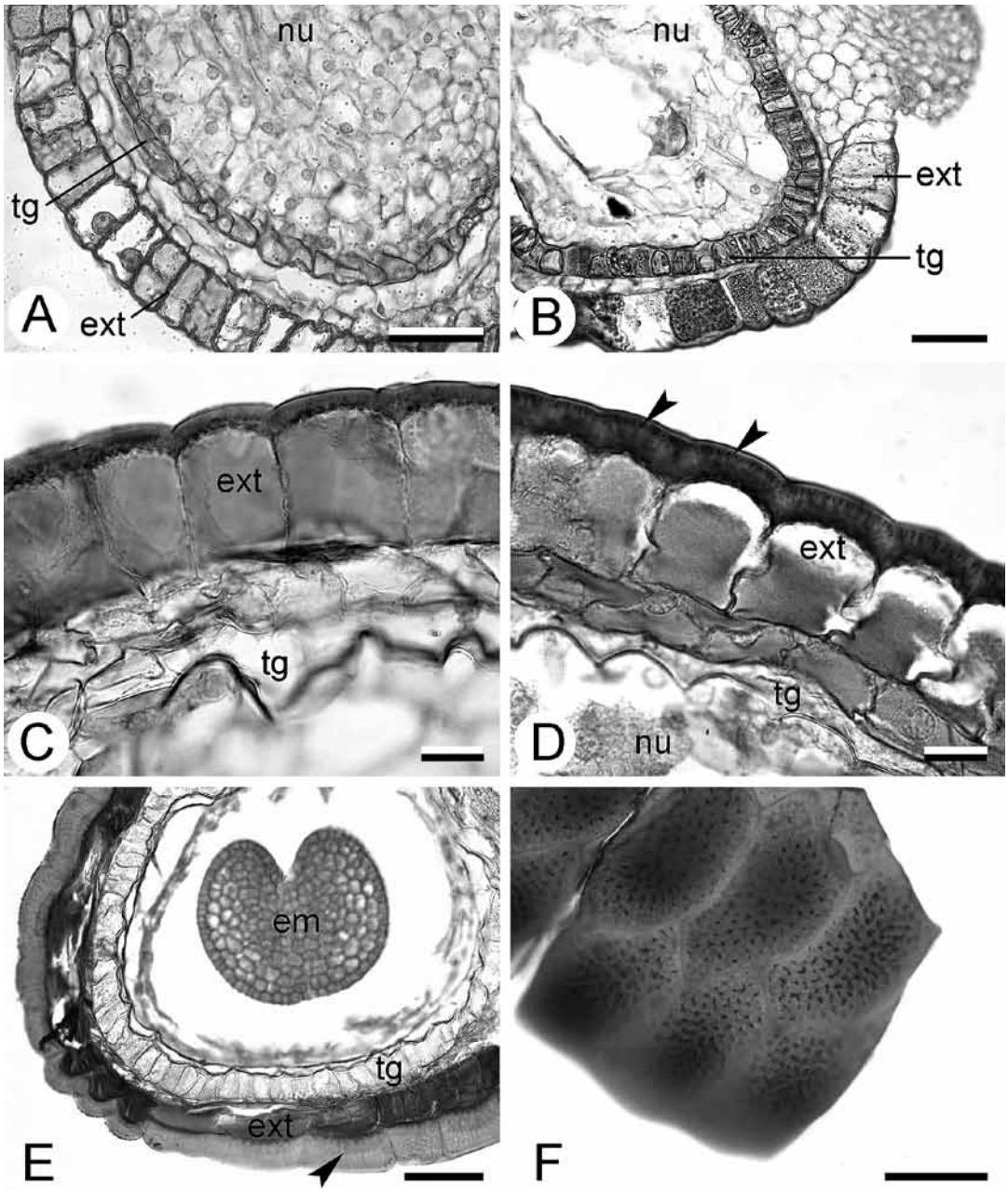

Figure 18. *T. paniculatum*, seed coat development. A–E – transverse sections. F – paradermal section showing pore canals within outer cell wall. em – embryo; ext – exotesta; nu – nucellus; tg – endotegmen. Arrowheads indicate pore canals within cell wall. Scale bars: in A–B, E–F = 50 µm; in C–D = 20 µm.

The species of the genus *Talinum* differ in ploidy level (Steiner 1944), inflorescence structure (Timonin 2005), pollen types (Nyananyo 1993), anatomy and fine sculpture of seeds (Nyananyo & Olowokudejo 1986) and fruit dehiscence mode (Galati 1986; Carolin 1987; Ferguson 2001; Veselova et al. 2011). We have revealed some additional differences between the species examined: Pollen grains of *T. paniculatum* are multicolpate, whereas *T. triangulare* produces multiporate pollen. Pollen grains of *T. triangulare* are larger, perhaps because of the polyploidy of this species (Steiner 1944).

Embryo development generally follows Solanad-type in both species but in *T. paniculatum*, the embryo *per se*, the hypophysis and even a part of the suspensor are formed by the cell *ca*, which is the distal cell of the 2-celled proembryo (Guignard 1965). In *T. triangulare*, both hypophysis and entire suspensor are derivatives of the cell *cb*, the basalmost cell of 2-celled proembryo. At

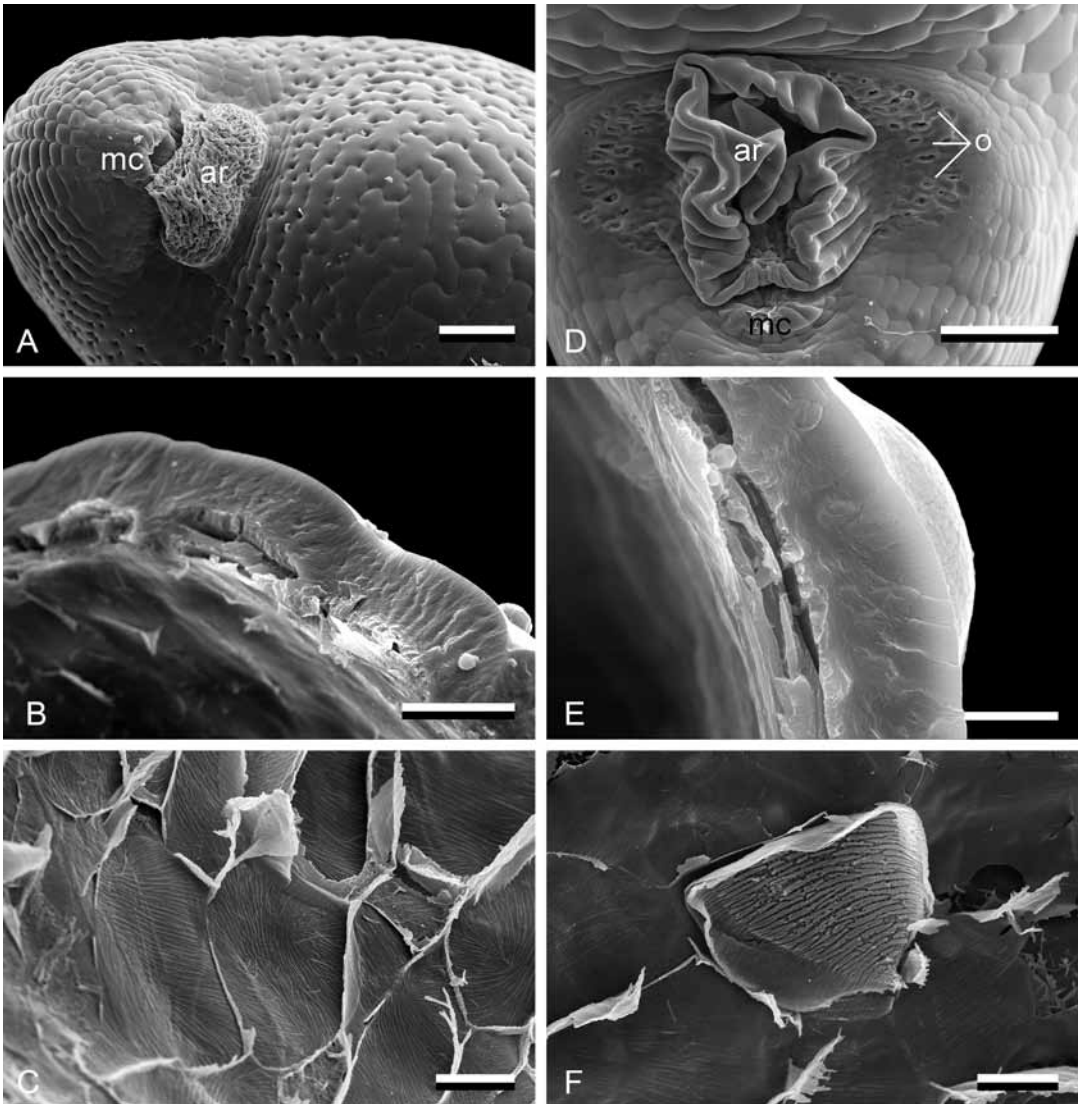

Figure 19. Seed coat surface and structure in mature seed (SEM). A–C – *T. paniculatum*. D–F – *T. triangulare*. A, D – seed, micropylar view. B, E– transversally dissected seed showing seed coat structure. C, F – endotegmen, surface view. ar – aril; mc – micropyle; o – omphalodium. Scale bars: in A, D = 100 μm; in B = 30 μm; in E–F = 10 μm.

the stage of late globular embryo, the species show different structure of the suspensor. The suspensor of *T. paniculatum* is mainly uniseriate, whereas that of *T. triangulare* consists of few rows of cells and has a massive base.

Although the seed coats are anatomically the same in two species concerned, they differ in fine sculpture. Seeds of *T. paniculatum* are almost smooth, but seeds of *T. triangulare* are clearly mammillate. Additionally, there are specific rimmed cells in the hilum area in *T. triangulare*. These cells apparently constitute an omphalodium here termed as 'structure regulating seed water balance'. The presence/absence of the omphalodium seems to be correlated with fruit dehiscence modes. *T. triangulare* demonstrates explosive capsule dehiscence. At the moment of fruit dehiscing, three capsule valves curve inwards and push releasing seeds away up to 0.5 m from the mother plant. Such autochoric seed dispersal is probably accompanied by zoochorous one. The latter is suggested on the base of presence of arils with voluminous proteins and lipids. The omphalodium apparently enables the released seed to intensify water intake for a faster germination. This could be of adaptive importance under conditions of semiarid habitats preferred by *Talinum*.

However, explosive fruit dehiscence is not typical of the genus. The capsules of *Talinum paniculatum* and a lot of other *Talinum* species dehisce gradually via formation of a set of slits, viz. three longitudinal dorsal and one basal circumscissile, which are accompanied by tangential splitting of the seed vessel wall resulting in three inner and three outer semivalves, respectively (Galati 1986; Carolin 1987; Ferguson 2001; Veselova et al. 2011). The outer ones immediately shed off, whereas the inner ones remain hanging on their dorsal bundles to form a kind of membranous container full of detached seeds. The seeds remain inside this container for a rather long period of time (for few weeks under laboratory conditions) because the slits and the basal orifice are too narrow in comparison to the seeds.

Such a specific fruit dehiscence is accompanied by unusual structure of the funicle. We hypothesize, that such slow seed dispersal can naturally be accelerated by small insects that get into the dehisced capsule attracted by detached funicle epidermis whose cells contain lipids. This hypothesis is supported by the fact that the aril of *T. paniculatum* lacks nutrients and thus cannot properly attract insects for zoochoric seed dispersal. Attractant-rich funicle epidermis separates from the seed and remains attached inside the capsule. Therefore, the zoochorous seed dispersal is unlikely in *T. paniculatum*.

Relatively long storage of the mature seeds inside the fruit apparently requires a mechanism preventing fast seed germination. Membranous inner semivalves are hardly able to keep seeds dry under the rain and thus delay their subsequent *in situ* germination. Meanwhile, the mechanisms of deep seed dormancy are rather disadvantageous under semiarid environments. Thus, we assume that in *T. paniculatum* the absence of an omphalodium as a specialized structure for water absorption can cause seed dormancy for the period of time to keep the seed ungerminated in the dehisced capsule. Due to the absence of an omphalodium, the rate of water absorption through the seed coat is decreased preventing precautious seed germination inside the capsule.

Acknowledgements

The authors are grateful to Dr Dmitry D. Sokoloff, Lomonosov Moscow State University, for critical reading of the manuscript and important suggestions, to Dr Elena M. Arnautova,

Komarov Botanical Institute of Russian Academy of Sciences (St Petersburg), and Dr Vladimir Kh. Pankin, Tsytsyn Main Botanic Garden of Russian Academy of Sciences (Moscow), for living plant material. We are indebted to the staff of the Laboratory of Scanning Electron Microscopy for their help with SEM studies.

References

Angiosperm Phylogeny Group [APG III] (2009): An update of the Angiosperm Phylogeny Group classification for the orders and families of flowering plants: APG III. – Bot. J. Linn. Soc. **161**: 105–121.

Bair A., Howe M., Roth D., Taylor R., Ayers T. & Kiger R.W. (2006): Portulacaceae. Purslane family. – Canotia **2**(1): 1–22.

Barykina R. P., Veselova T. D., Devyatov A. G., Dzhalilova K. Kh., Ilyina G. M. & Chubatova N. V. (2004): Botanical microtechnique manual. Principles and methods. – Moscow: Moscow Univ. Press. [In Russian]

Batygina T. B. (1983): Family Portulacaceae. – In: Yakovlev M. S. [ed.]: Comparative embryology of flowering plants: 26–32. – Leningrad: Nauka Publ. [In Russian]

Brummitt R. K. (1978): Report of the Committee for Spermatophyta, 21. – Taxon **27**(5/6): 543–546.

Carolin R. (1987): A review of the family Portulacaceae. – Austral. J. Bot. **35**(4): 382–412.

Cooper D. C. (1940): Macrosporogenesis and embryology of *Portulaca oleracea*. – Amer. J. Bot. **27**(5): 326–330.

De Candolle A. P. (1828): Prodromus systematis naturalis regni vegetabilis, sive enumeratio contracta ordinum, generum, specierumque plantarum huc usque cognitarum, juxta methodi naturalis normas digesta. Pars 3. Sistens Calyciflorarum Ordines XXVI. – Paris: Treuttel et Würtz.

Ferguson D. J. (2001): *Phemeranthus* and *Talinum* (Portulacaceae) in New Mexico. – New Mexico Botanist **20**: 1–7.

Galati B. (1986): Ontogenia del fruto de *Talinum paniculatum* (Jacq.) Gaertn. (Portulacaceae). – Parodiana **4**: 12–131.

Guignard J. L. (1965): Embryogénie des Portulacacées. Développement de l'embryon chez le *Talinum patens* Willd. – Compt. Rend. Acad. Sci. Paris **261**(25): 5599–5601.

Gusev Yu. D. (1980): Portulacaceae. – In: Takhtajan A. L. [ed.]: Plant life. Vol. 5: 361–263. – Moscow: Prosveschenie Publ. [In Russian]

McNeill J. (1974): Synopsis of a revised classification of the Portulacaceae. – Taxon **23**(5/6): 725–728.

McNeill J. (1977): Proposal to conserve 2406 *Talinum* Adanson with the type *T. triangulare* (Jacq.) Willd. – Taxon **26**(1): 147.

Nyananyo B. L. (1993): Pollen morphology in the Portulacaceae (Centrospermae). – Folia Geobot. Phytotax. **27**: 387–400.

Nyananyo B. L. & Olowokudejo J. D. (1986): Taxonomic studies in the genus *Talinum* (Portulacaceae) in Nigeria. – Willdenowia **15**: 455–463.

Nyffeler R. & Eggli U. (2010): Disintegrating Portulacaceae: A new familial classification of the suborder Portulacineae (Caryophyllales) based on molecular and morphological data. – Taxon **59**(1): 227–240.

Pax F. (1889): Portulacaceae. – In: Engler A. & Prantl K. [eds]: Die natürlichen Pflanzenfamilien nebst ihren Gattungen und wichtigeren Arten insbesondere den Nutzpflanzen. 3. Teil 1. Abt. b: 51–60. – Leipzig: W. Engelmann.

Plisko M. A. (1991): Family Portulacaceae – In: Takhtajan A. L. [ed.]: Comparative seed anatomy. Vol. 3. Dicotyledones. Caryophyllidae – Dilleniidae: 28–33. – Leningrad: Nauka. [In Russian]

von Poellnitz K. (1934): Monographie der Gatting *Talinum* Adans. – Rep. spec. nov. regni vegetab. **35**: 1–34.

Steiner E. (1944): Cytogenetic studies on *Talinum* and *Portulaca*. – Bot. Gaz. **105**(3): 374–379.

Stevens P. F. (2008): Angiosperm phylogeny website. Version 9, June 2008 [and more or less continuously updated since]. – Electronic resource; mode of access: http://www.mobot.org/MOBOT/research/APweb/

Takhtajan A. (1987): Systema Magnoliophytorum. – Leningrad: Nauka.[In Russian]

Timonin A. C. (2005): Cymoid evolution resulting in (closed) thyrse: *Talinum* Adans. (Portulacaceae) versus Wilhelm Troll. – Wulfenia **12**: 1–19.

Veselova T. D., Dzhalilova Kh. Kh. & Timonin A. C. (2011): Atypical fruit of *Talinum triangulare* (Jacq.) Willd., the type species of the genus *Talinum* (Talinaceae, former Portulacaceae). – Wulfenia **18**: 15–35.

Veselova T. D. & Timonin A. C. (2009): *Pleuropetalum* Hook. f. is still an anomalous member of Amaranthaceae Juss. An embryological evidence. – Wulfenia **16**: 99–116.

Vishenskaya T. D. (1991): Family Cactaceae. – In: Takhtajan A. L. [ed.]: Comparative seed anatomy. Vol. 3. Dicotyledones. Caryophyllidae – Dilleniidae: 41–57. – Leningrad: Nauka. [In Russian]

Address of the authors:

Dr Tatiana D. Veselova
Khalima Kh. Dzhalilova
Dr Margarita V. Remizova
Prof. Dr Alexander C. Timonin
Department of Higher Plants
Faculty of Biology
Lomonosov Moscow State University
Vorobyevy Gory 1 (12)
119992 Moscow
Russia
E-mail: timonin58@mail.ru